

NUMERICAL METHOD FOR ESTIMATING THE SIZE OF CHAOTIC REGIONS
OF PHASE SPACE

Frank S. Henyey

Center for Studies of Nonlinear Dynamics[†]

La Jolla Institute

10280 N. Torrey Pines Rd, Suite 260

La Jolla, Ca 92037

and

Neil Pomphrey

Princeton Plasma Physics Laboratory

P.O. Box 451

Princeton, New Jersey 08544

ABSTRACT

A numerical method for estimating irregular volumes of phase space is derived. The estimate weights the irregular area on a surface of section with the average return time to the section. We illustrate the method by application to the stadium and oval billiard systems and also apply the method to the continuous Hénon-Heiles system.

[†]Affiliated with the University of California, San Diego.

I. INTRODUCTION

Here, we describe a simple numerical method for estimating the irregular volumes of phase space of nonintegrable Hamiltonian systems. The method requires calculating a surface of section and monitoring the time intervals between returns to the section. The stochastic area of the section weighted by the average return time gives the estimate for the irregular volume.

It is useful to motivate our results by considering the dynamics of billiard systems. These are discontinuous Hamiltonian systems defined by a particle moving freely inside an enclosure whose boundaries have some specified shape. By choosing different shapes of boundary, it is possible to exhibit the full range of behavior obtained by continuous Hamiltonian systems, from integrable (ellipse) to nonintegrable (oval) behavior as well as to ergodic (stadium) and more strongly chaotic behavior.¹⁻⁴ In addition, the infinite potentials at the boundaries of billiard enclosures can lead to so-called almost-integrable (pseudointegrable) behavior not seen in continuous systems.⁵⁻⁷

Consider the motion of a billiard ball in an ergodic enclosure, such as the famous stadium.³ On the average, a nonperiodic orbit of the system spends equal time in equal volumes of phase space. As the ball bounces around the enclosure, it describes a sequence of connected chords of differing lengths. We focus on the average chord length. In Sec. II we show that for motion within a two-dimensional ergodic enclosure, the average bounce length between collisions equals $\pi A/P$, where A is the area and P the perimeter of the enclosure. This result is independent of details of shape, and is identical to a well-known formula of geometric probability⁸⁻¹⁰: Crofton proved in 1885 that with an appropriate choice of measure, a random set of unconnected chords of an arbitrary two-dimensional domain have an average length of $\pi A/P$.¹¹ A

three-dimensional analogue of this result is familiar in architectural acoustics where to a reasonable approximation the reverberation time of an auditorium is proportional to the mean-free path of sound. For an ergodic auditorium this is $4V/S$ where V is the volume and S is the surface area.¹²

In Sec. III we illustrate the convergence of $\langle L \rangle$ to its predicted value for a stadium billiard. The result is generalized in Sec. IV to the case of continuous Hamiltonian systems and a formula is developed for the average time interval $\langle t \rangle$ between crossings of a trajectory with a surface of section. The formula for $\langle t \rangle$ is obtained by assuming ergodicity over the entire energy shell. If we assume for an approximation that the irregular regions of phase space of nonintegrable Hamiltonian systems are ergodic, we suggest a method of using the basic formula for $\langle t \rangle$ to estimate the volume of the irregular regions. This volume is given by weighting the area of the stochastic regions of a surface of section with the average crossing time.

As a test case for the proposed method, we consider in Sec. V the dynamics of an oval billiard. Our reason for choosing this nonintegrable billiard system as a test case instead of a continuous system is that the phase space structure of the oval billiard is sufficiently simple to allow an accurate calculation of the true irregular volume, so that we have a value with which to compare. The agreement is found to be good. Finally, in Sec. VI, we apply the method to estimate the volume of the irregular region of phase space of the continuous Hénon-Heiles system.¹³

II. AVERAGE BOUNCE LENGTH FOR CHAOTIC BILLIARDS

Consider the motion of a billiard ball moving with unit speed inside an "ergodic enclosure" (see Fig. 1a). We ask for the probability that during a small time interval Δt , the billiard ball will collide with the wall. Since

the ball travels unit distance in unit time, it will hit a wall during Δt if it is within a distance Δl of the wall, along the direction of motion. Clearly, the probability of a collision is

$$P(\text{hit}) = \Delta l / \langle L \rangle \quad (1)$$

where $\langle L \rangle$ is the average length traveled by the ball between bounces. No reference has been made to dynamics. However, we can calculate the same probability in a way that does refer to the dynamics. To do this, let us specify the position of the ball relative to the wall by the perpendicular separation distance x , and by the angle of incidence θ (see Fig. 1b). The time limit allowed for a collision, and the constancy of speed implies an upper limit to a distance along the direction of motion if a "hit" is to occur. In particular,

$$0 < \frac{x}{\cos \theta} < \Delta l \quad (2)$$

Consistent with the assumption that the motion is ergodic, we assume that all angles of incidence θ are equally likely. Then the probability of a hit in time Δt is

$$P(\text{hit}) = \frac{1}{2\pi} \int_{-\pi}^{\pi} d\theta \int_0^{\Delta l \cos \theta} p(x) dx \quad (3)$$

where $p(x)dx$ is the probability density for x . Since x is small, $p(x)$ is independent of position along the boundary and is given by

$$p(x)dx = \frac{1}{A} dx \int d(\text{length along boundary})$$

$$= \frac{P}{A} dx \quad (4)$$

Insertion in Eq. (3) yields

$$P(\text{hit}) = \frac{P}{\pi A} \Delta l \quad (5)$$

Expressions (1) and (5) describe probabilities for the same event and may therefore be equated. We are led to the result

$$\langle L \rangle = \pi A / P \quad (6)$$

for the average bounce length. The detailed shape of the enclosure is irrelevant. The only requirement is that the motion is ergodic.

In the next section, we demonstrate the validity of Eq. (6) with a numerical experiment.

III. ILLUSTRATION: THE STADIUM

The dynamics of a stadium billiard is known to be ergodic (in fact, a K-system).^{3,4} This enclosure has boundaries defined by two opposing semi-circles of radius r , joined with tangential straight lines of length $2d$. Symmetry implies the dynamical equivalence of the 1/4-stadium shown in Fig. 2. With the choice $d = 1$, $r = 1$ a trajectory can describe chord lengths of between $L_{\min} = 0$, corresponding to grazing collisions, and $L_{\max} = \sqrt{5} \approx 2.36$ corresponding to a bounce between the top left and bottom right corners. (This maximum length orbit of the 1/4-stadium is equivalent to the unstable diamond orbit of the full stadium.) For the given dimensions, we have $A = 1 + \pi/4$ and $P = 4 + \pi/2$, which obtain $\langle L \rangle = 1.0068\dots$ from Eq. (6).

Figure 3 shows the results of a numerical experiment where three trajectories with different initial conditions are followed for 10^6 bounces. Convergence toward zero is shown of the difference between the calculated average bounce length and the predicted value $\pi A/P$. The error bar spans data which lies within 1% of the true value $\langle L \rangle = 1.0068\dots$. A detailed discussion of the convergence of $\langle L \rangle$ will not be given here. The longest time scale for the convergence is determined by the Poincaré recurrence time. Major excursions from a monotonic convergence of $\langle L \rangle$ occur when trajectories linger near an unstable or neutrally stable periodic orbit, such as the $L = 2$ unstable orbit labelled AB in Fig. 2, or the $L = 1$ neutrally stable orbit AD.

To see how a prediction of the value of $\langle L \rangle$ can be made useful, consider first a trivial experiment: The expression for average bounce length for the stadium can be written as

$$\frac{\pi A}{P} = \frac{\pi r}{2} \frac{(4a+\pi)}{(4+4a+\pi)} = \langle L \rangle \quad , \quad (7)$$

where $a = d/r$ is the aspect ratio. By following the billiard dynamics we can obtain an estimate for the right-hand side $\langle L \rangle$. Then Eq. (7) can be regarded as an algebraic equation for the aspect ratio a . Thus, the trajectory data can be inverted to obtain information about the geometry of the enclosure.

Clearly, the above example is of limited interest. However, it is straightforward to generalize the results of Sec. II to continuous Hamiltonian systems. The quantity $\langle L \rangle$ generalizes to the average time between intersections with a surface of section, and we will argue that the expression for average time can be used as an inversion scheme to estimate irregular volumes of phase space.

IV. GENERALIZATION TO CONTINUOUS SYSTEMS

Consider a continuous Hamiltonian system $H(\vec{q}, \vec{p})$ with N degrees of freedom. Assume that the system is ergodic so that system trajectories spend equal times in equal volumes of phase space. Figure 4 displays a cartoon of a trajectory pictured near a surface of section $S(\vec{q}, \vec{p}) = 0$. The section need not be a Poincaré section. As in the billiard problem, we ask for the probability that during some small time interval Δt the trajectory crosses the chosen section. Two ways of writing this probability are:

$$P(\text{cross}) = \frac{\Delta t}{\langle t \rangle} \quad , \quad (8)$$

where $\langle t \rangle$ is the average time interval between crossings, and

$$P(\text{cross}) = \frac{\int d\vec{q} d\vec{p} \delta[E-H(\vec{q}, \vec{p})] (ds/dt) \delta(s) \Delta t}{\int d\vec{q} d\vec{p} \delta(E-H)} \quad (9)$$

Equation (9) is entirely analogous to Eqs. (3-5) but uses canonical coordinates and an arbitrary section. It expresses the probability of crossing S in a time Δt as the phase space integral over the energy shell (region available to the trajectory) of the velocity through the chosen section, integrated for the time interval Δt , normalized by the volume of the energy shell. Equating the two probabilities yields an expression for the average time interval between crossings of trajectory with the section $S(\vec{q}, \vec{p}) = 0$:

$$\langle t \rangle = \frac{\int d\vec{q} d\vec{p} \delta[E-H(\vec{q}, \vec{p})]}{\int d\vec{q} d\vec{p} \delta(E-H) \dot{S} \delta(s)} \quad (10)$$

The section S can be made into a Poincaré section by canonically transforming

the coordinates (\vec{q}, \vec{p}) into (\vec{s}, \vec{r}) , with $s_1 = S$. The denominator of Eq. (10) becomes

$$\int_{j \neq 1} ds_j dr_j ,$$

the Poincaré invariant for the remaining variables. Thus, the average $\langle t \rangle$ is simply the ratio of the volume of the energy shell to the area of the Poincaré section. It is easy to show that Eq. (10) reduces to Eq. (6) for billiards when the section S is chosen to be the boundary of the enclosure.

The result (10) was obtained by assuming the system is ergodic over the entire energy shell. However, typical Hamiltonian systems are nonintegrable and a region of chaos (irregular regions) fills restricted volumes of phase space.¹⁴ To make progress, we invoke the ergodic theorem¹⁵ which ensures that the motion of an irregular trajectory of a nonintegrable system is ergodic over some restricted volume V_I of phase space. Then Eq. (10) is written (for a Poincaré section) as

$$V_I = \langle t \rangle A_I . \quad (11)$$

Thus, to estimate the volume of the irregular region, one chooses a Poincaré section and integrates the equations of motion to obtain points on the section and time intervals between arrivals. When the average return time has converged satisfactorily, the integrations are halted and the area of the stochastic sea on the section is estimated. Finally, the area and the average time are multiplied to obtain the irregular volume.

Although we have formulated (and applied, see Sec. VI) the technique for continuous Hamiltonian systems, it is appropriate to test the procedure on the

nonintegrable problem of billiards in an oval enclosure. Since the dynamics follows from the application of the laws of reflection, much of the phase space can be understood using simple trigonometry. This makes possible a good estimate of the "exact" irregular volume which can be compared with the numerical results from Eqs. (10) and (11). We do this in the next section.

V. A TEST CASE: THE OVAL BILLIARD

The construction of an oval enclosure is shown in Fig. 5. A point O_1 on the vertical bisector of a unit square is the center of a circle which touches the square at two corners P and P' . The radius O_1P intersects the horizontal bisector of the square at O_2 , which is the center of a second circle with radius O_2P . By construction, the two circles have a common tangent at P so a smooth curve can be drawn from y through P to X . Reflection of the curve through the x and y axes obtains the oval boundary. The ratio of the radii of the two circles is an important parameter for the dynamics of the oval billiard. By varying $\alpha = O_1P/O_2P$ from 1 to ∞ , the oval can be continuously deformed from the integrable circle to the ergodic stadium. The dynamics of an oval billiard was first studied by Benettin and Strelcyn.³

Consider the motion of a billiard ball which moves with unit speed inside the 1/4-oval OYPX with $\alpha = 10$. Figure 6 shows the Poincaré surface of section v_x versus x for $y = 0$: For each collision of the ball with the straight bottom edge we plot the position along the edge (x) and the tangential velocity (v_x). On this section we see a set of nested level curves centered on an elliptic fixed point at $x = 0$, $v_x = 0$. The fixed point corresponds to a stable two-bounce periodic orbit generated by an initial velocity vector lying along the vertical radius of the large circle. The family of tori which surrounds the fixed point is generated by trajectories which also lie along

radius vectors; however, these radius vectors have a finite slope of v_y/v_x . If we follow one of these trajectories, we find that it explores the region of the 1/4 oval to the left of the initial radius vector; it never explores the region to the right. An initial condition corresponding to a velocity which lies along the common radius vector of the two circles O_2P , leads to a "limiting" trajectory which explores all of the left circle but none of the right.

Suppose we perturb the limiting torus by further decreasing the velocity gradient, keeping the initial x at point O_2 . The billiard ball now experiences collisions with the small circle. However, there are many more collisions with the large circle, whose stabilizing influence wins and the tori are preserved. Eventually, however, when v_y/v_x is sufficiently small there are enough destabilizing bounces off the small circle to result in torus destruction and the stochastic sea of Fig. 6. The last surviving torus was found numerically to correspond to $v_y/v_x = 7.9$.

Having found a good approximation to the last big torus of the oval, its volume can be determined. For this, we numerically integrate the phase space volume element over the torus, using trajectory data to calculate the regular volume

$$V_R = \int_{\text{last torus}} dx dy dv_x dv_y \delta(1 - v_x^2 - v_y^2) \quad . \quad (12)$$

The irregular volume V_I is the complement of V_R with the energy shell volume V_E . Thus

$$V_I = V_E - V_R$$

$$= \pi A - 0.506$$

$$= 4.917 \quad . \quad (13)$$

It is with this number we wish to compare the estimate Eq. (11) of volume based on return time to a surface of section.

The choice of section is unimportant, but the given interpretation for torus breakdown suggests a better section than that used in Fig. 6, namely v_y versus y for $x = 1$. This section is shown in Fig. 7a and it is apparent why this was a good choice; to a good approximation the section is entirely stochastic. The only evidence of islands is at the top right-hand corner. A magnification of this region is shown in Fig. 7b, where islands are labelled with the initial value of v_y/v_x . If the island region is ignored (it counts for less than 0.5% of the area of the section), we obtain for the denominator of Eq. (10)

$$A_I = \int_I dx dy dv_x dv_y \delta(1 - v_x^2 - v_y^2) v_x \delta(x - 1)$$

$$= 1 \quad . \quad (14)$$

To estimate the irregular volume from Eq. (11) we now need $\langle t \rangle$. Figure 8 shows the convergence of $\langle t \rangle$ for the oval billiard with $\alpha = 10$. Data from five initial conditions, show that the convergence of $\langle t \rangle$ is not without problems. Each of the runs shows a number of "events" where $\langle t \rangle$ significantly increases. These occur when a trajectory approaches close to a torus. In the configuration space of the oval this corresponds to the orbit executing many

consecutive bounces on the large circle. We have made no attempt to understand the distribution of the frequency and duration of these events. Without this knowledge we can do no better than to calculate $\langle t \rangle$ as the average over all five runs after 10^6 bounces. This gives $\langle t \rangle = 4.922$. Hence, our estimate given by Eqs. (10) or (11) of the irregular volume is

$$V_I = 1.0 \times 4.922 \quad , \quad (15)$$

which agrees well with the value 4.917 obtained by the independent calculation. Furthermore, the estimate was easy to calculate, whereas the independent calculation was only straightforward for this billiard problem where obtaining a good guess of the last torus was simple.

VI. APPLICATION TO THE HÉNON-HEILES SYSTEM

The Hénon-Heiles Hamiltonian is defined as

$$H = T(\dot{x}, \dot{y}) + V(x, y)$$

where

$$T = 1/2(\dot{x}^2 + \dot{y}^2)$$

and

$$V = 1/2(x^2 + y^2) + x^2y - 1/3y^3 \quad (16)$$

are the kinetic and potential energies of the system.¹³ If $H < E_c = 1/6$, the phase space of the system is bounded. Hénon and Heiles found that system trajectories with $H < 3/4E_c$ are mainly confined to invariant tori, but as H is

increased toward the escape value, E_c , the phase space becomes predominantly irregular.

Figure 9 shows 2000 points on a surface of section for the Hamiltonian (16) at the energy $H = 0.9999E_c$. The section is \dot{x} versus x at $y=0$ with the restriction $\dot{y} > 0$. Points were generated by a single trajectory using the initial conditions $x=0$, $y=0.3$, $\dot{y}=0.3$, with \dot{x} determined by the value of H . Apart from two crescent regions extending to the circular boundary of the classically allowed region (whose radius is $1/\sqrt{3}$), and a small circular region near $\dot{x} = x = 0$, the section is covered by a stochastic sea. A simple estimate of the stochastic area on the section is obtained by "counting squares" and gives $A_I = 0.92$.

Using the same trajectory data that gave Fig. 9, the average time between successive intersections with the surface of section was calculated, and is shown in Fig. 10. The results have been smoothed by averaging over intervals containing 25 intersections; therefore, the figure appears as a histogram. The average time between crossings with the section is seen to converge to $\langle t \rangle = 7.80$. Thus, from equation (11), we obtain an estimate for the volume of the energy shell explored by the irregular trajectory which gave rise to the surface of section shown in Fig. 9:

$$V_I = \langle t \rangle A_I = 7.80 \times 0.92 = 7.18 \quad . \quad (17)$$

The total volume of the energy shell of the Hénon-Heiles system is

$$V_E = \frac{2\pi \int dx dy}{1/2(x^2 + y^2) + x^2 y - 1/3 y^3 < H}$$

$$= 4\pi/3 \int_{r_1}^{r_2} dy \left[\frac{(y-r_1)(y-r_2)(y-r_3)}{y + 1/2} \right]^{1/2}$$

where r_1, r_2, r_3 are the roots of $y^3 - \frac{3}{2}y^2 + 3H = 0$. Therefore,

$$r_1 = \frac{1}{2} + \cos \frac{\phi + 2\pi}{3}$$

$$r_2 = \frac{1}{2} + \cos \frac{\phi + 4\pi}{3}$$

and

$$r_3 = \frac{1}{2} + \cos \frac{\phi}{3},$$

where

$$\phi = 2\sin^{-1} \sqrt{H/E_c}. \quad (18)$$

Clearly, the volume of the energy shell at $H = 0.9999 E_c$ is accurately estimated from the formulae (18) by writing $H/E_c = 1$. This obtains $V_H = 3/3\pi/2 = 8.16$. Thus, the estimate for the irregular volume given by equation (17) is that 88% of the available phase space is stochastic.

CONCLUSIONS

A straightforward numerical method has been presented for estimating the size of irregular volumes of phase space. The estimate weights the irregular area on a surface of section with the average return time to the section. The method, therefore, uses information that is readily available if a surface of section has been calculated.

ACKNOWLEDGMENTS

The connection of this work with the field of geometrical probability was pointed out to us by Professor Mark Kac, with whom we enjoyed many wonderful conversations on this and other topics. This work was supported by U.S. Department of Energy Contract No. DE-AC02-76-CHO-3073 and in part by internal La Jolla Institute funds.

REFERENCES

- ¹G.D. Birkhoff, Dynamical Systems (American Mathematical Society, Providence, RI, 1927).
- ²M.V. Berry, Eur. J. Phys. 2, 91-102 (1981).
- ³G. Benettin and J.M. Strelcyn, Phys. Rev. A17, 773-785 (1978).
- ⁴L.A. Bunimovich, Funct. Anal. Appl. 8, 254-255 (1974); Commun. Math. Phys. 65, 259-312 (1979).
- ⁵A.N. Zemlyakov and A.B. Katok, Math. Notes 18, No. 1-2 760-764 (1975).
- ⁶A. Hobson, J. Math. Phys. (N.Y.) 16, 2210-2214 (1975).
- ⁷P.J. Richens and M.V. Berry, Physica 2D 495-512 (1981).
- ⁸L.A. Santalo, "Integral Geometry and Geometric Probability," Encyclopedia of Mathematics and its Applications I, (Addison-Wesley, Reading, MA, 1976).
- ⁹H. Solomon, Geometric Probability (S.I.A.M., Philadelphia, PA, 1978).
- ¹⁰M.G. Kendall and P.A.P. Moran, Geometrical Probability (Griffin, London, 1963).
- ¹¹M.W. Crofton, "Probability," Encyclopedia Britannica, 9th Ed., Vol. 19 p. 768-788, 1885.
- ¹²W.B. Joyce, J. Acoust. Soc. Am. 58, 643-655 (1975).
- ¹³M. Hénon and C. Heiles, Astron. J. 69, 73-79 (1964).
- ¹⁴M.V. Berry, A.I.P. Conference Proceedings No. 46, 16-120 (1978).
- ¹⁵J.-P. Eckmann and D. Ruelle, Rev. Mod. Phys. 57, 617-656 (1985).

FIGURE CAPTIONS

- Fig. 1(a) Fictitious ergodic enclosure of area A and perimeter P . A segment of a trajectory is shown and (b) A snapshot of the motion. The ball is a distance Δl from the wall along the direction of motion. (x, θ) labels the ball's location at the time of the snapshot. Since Δl is assumed to be small, the wall appears to be flat.
- Fig. 2 The "stadium," showing orbits of minimum (---) and maximum (— — —) length. Computations are done in the 1/4-stadium ABCD.
- Fig. 3 Convergence of $\langle L \rangle$ to the predicted value $\pi A/P$ for three trajectories (, • , and x) of the stadium billiard. The error bar shows convergence to 1% accuracy.
- Fig. 4 A trajectory of $H(\dot{q}, \dot{p}) = E$ as it approaches and crosses the section $S(\dot{q}, \dot{p}) = 0$. Poincaré recurrence and ergodicity guarantee such a crossing.
- Fig. 5 Construction of Benettin and Strelcyn's oval enclosure. O_1 and O_2 are centers of curvature for circle arcs which join smoothly at P .
- Fig. 6 Surface of section $y = 0$ for oval with $\alpha = 10$. Initial conditions A-D lie along radius vectors of the large circle and have $v_y/v_x = 1000, 100, 50, 10$ resp. Trajectory E has initial x at point O_2 with $v_y/v_x = 7.8$.

- Fig. 7 Magnification of island region of Fig. 7a. Trajectories are labeled with initial v_y/v_x .
- Fig. 8 Average return time to section $x = 0$ for oval with $\alpha = 10$. Initial conditions for trajectory data are $v_y/v_x = 7.8, 7.5, 7.0, 6.0, 3.0$.
- Fig. 9 Surface of section \dot{x} vs x ; $y = 0, \dot{y} > 0$ for Hénon-Heiles system. $H = 0.16665$, 2000 points are shown.
- Fig. 10 Average time between successive returns to the surface of section. The trajectory and section are the same as in Fig. 9.

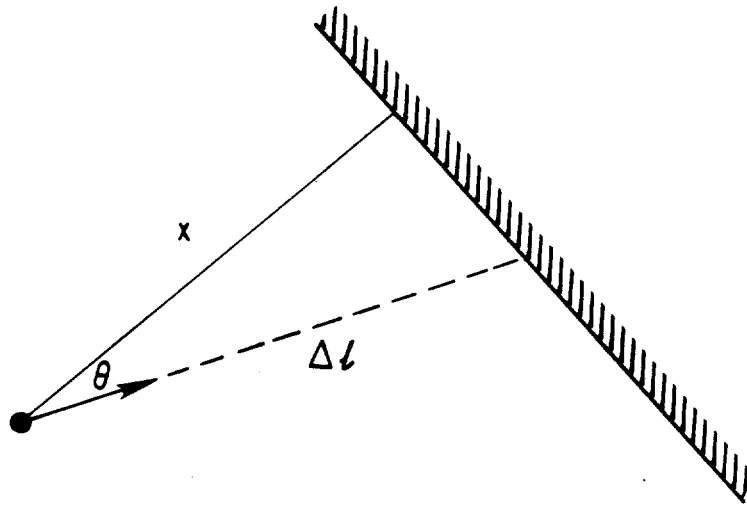
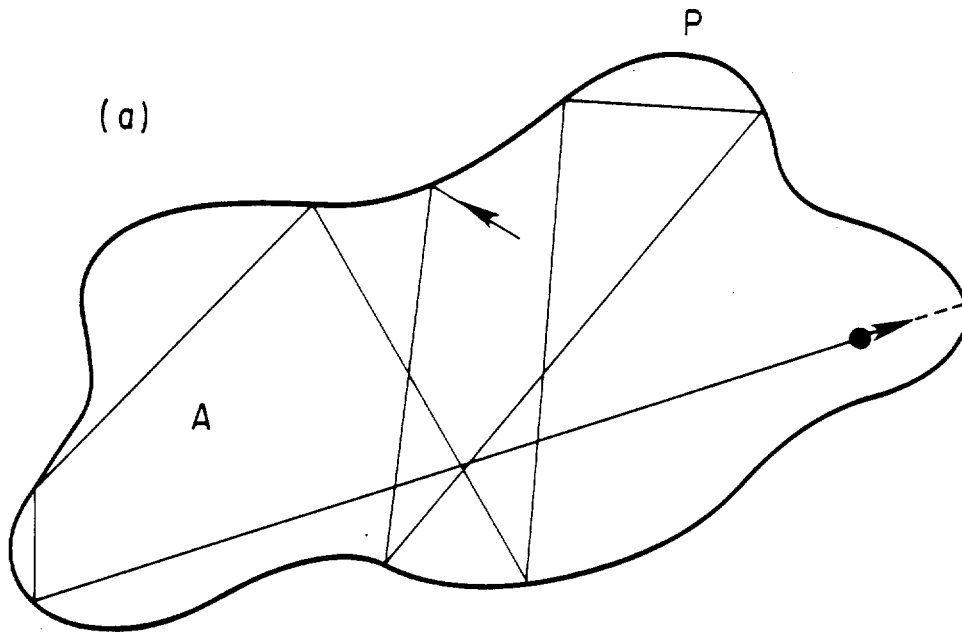


Fig. 1

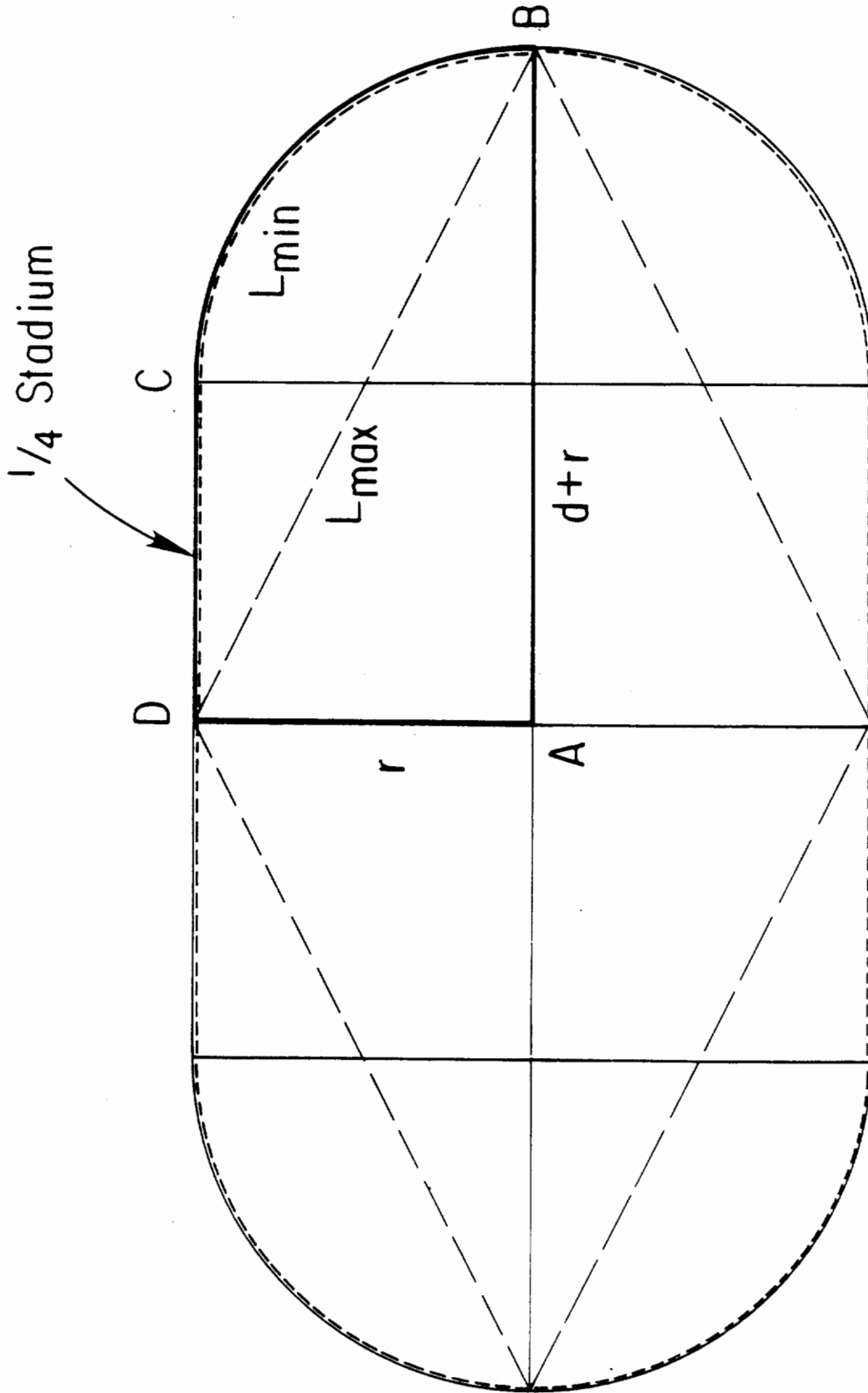


Fig. 2

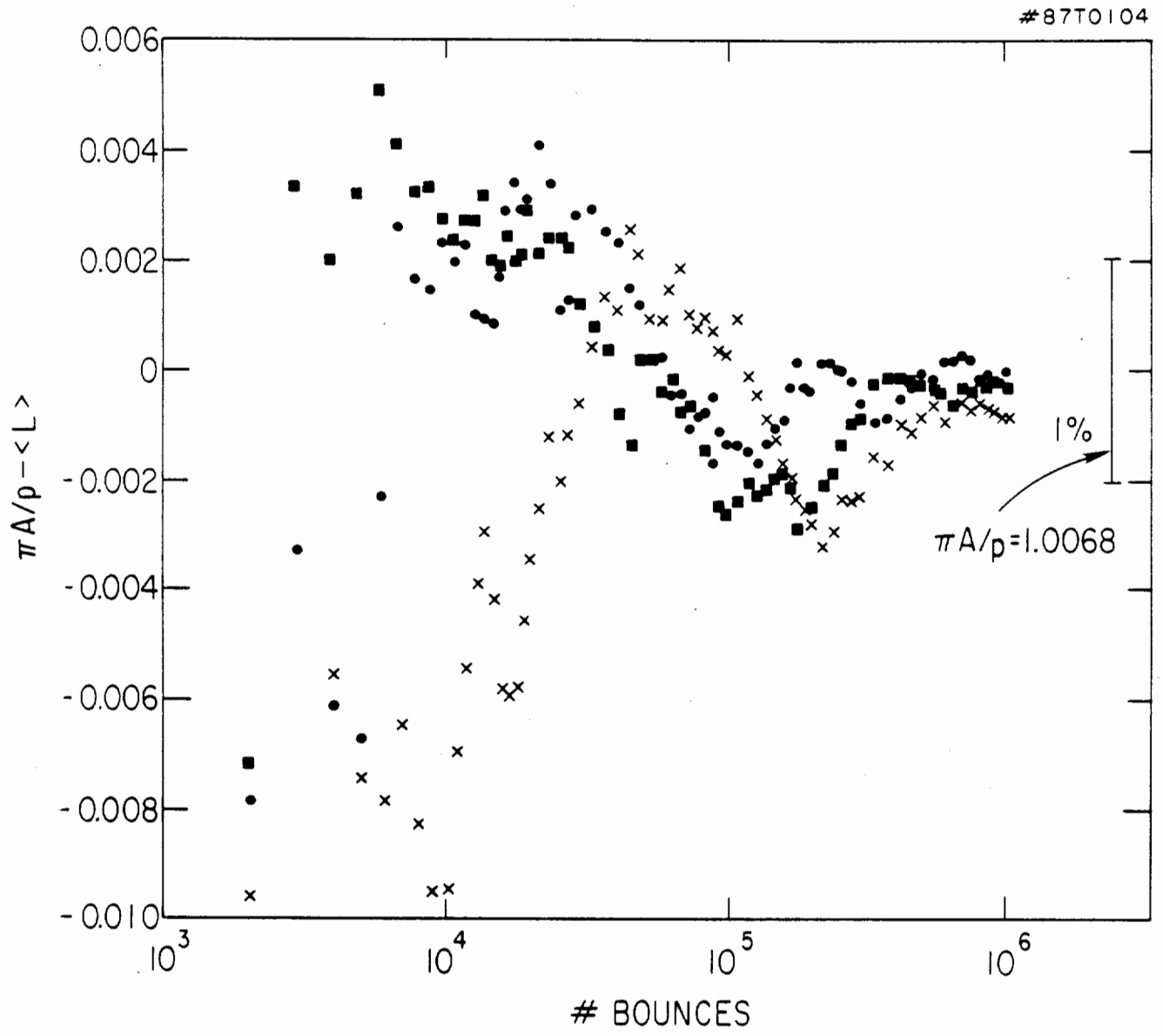


Fig. 3

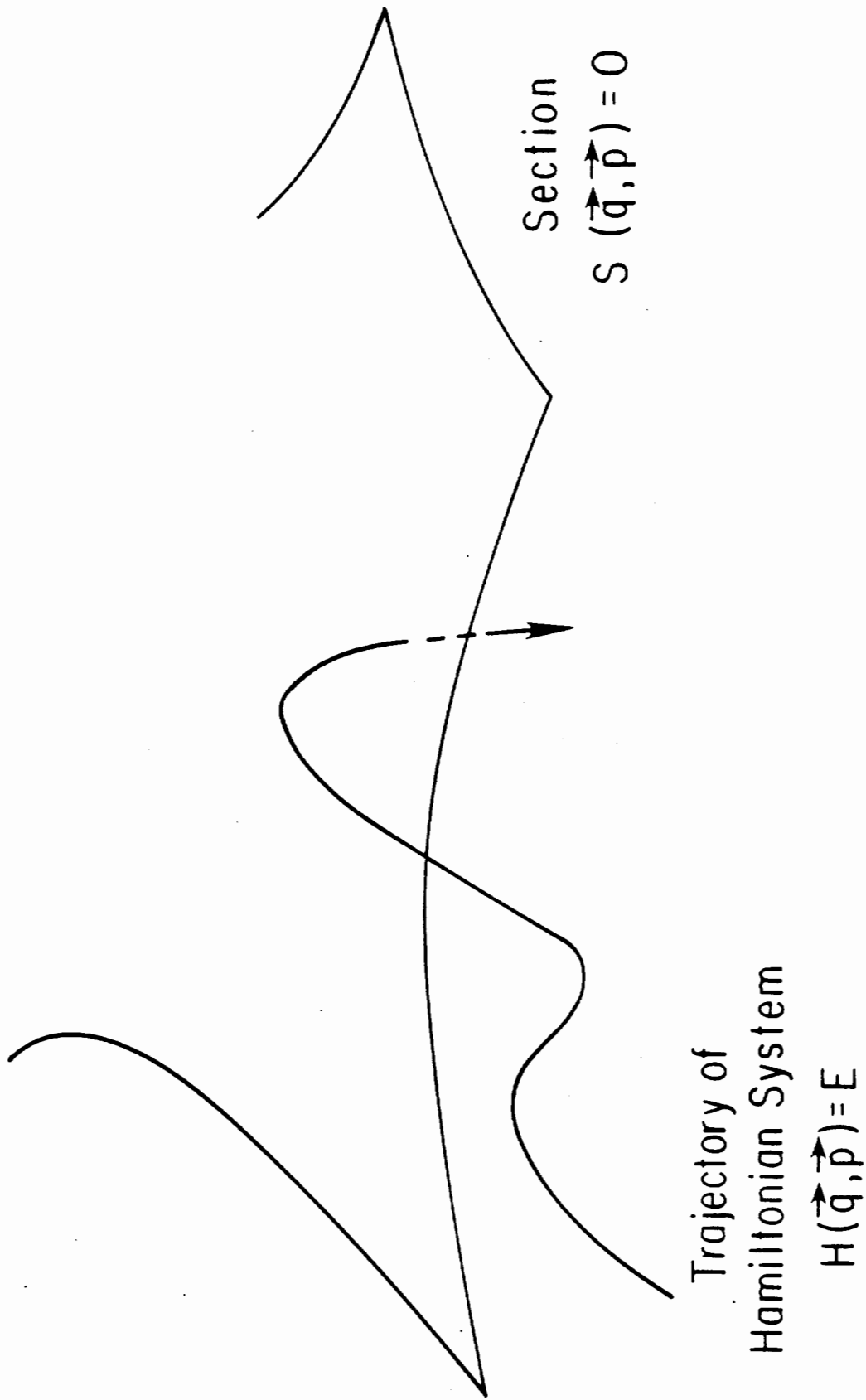


Fig. 4

#87T0105

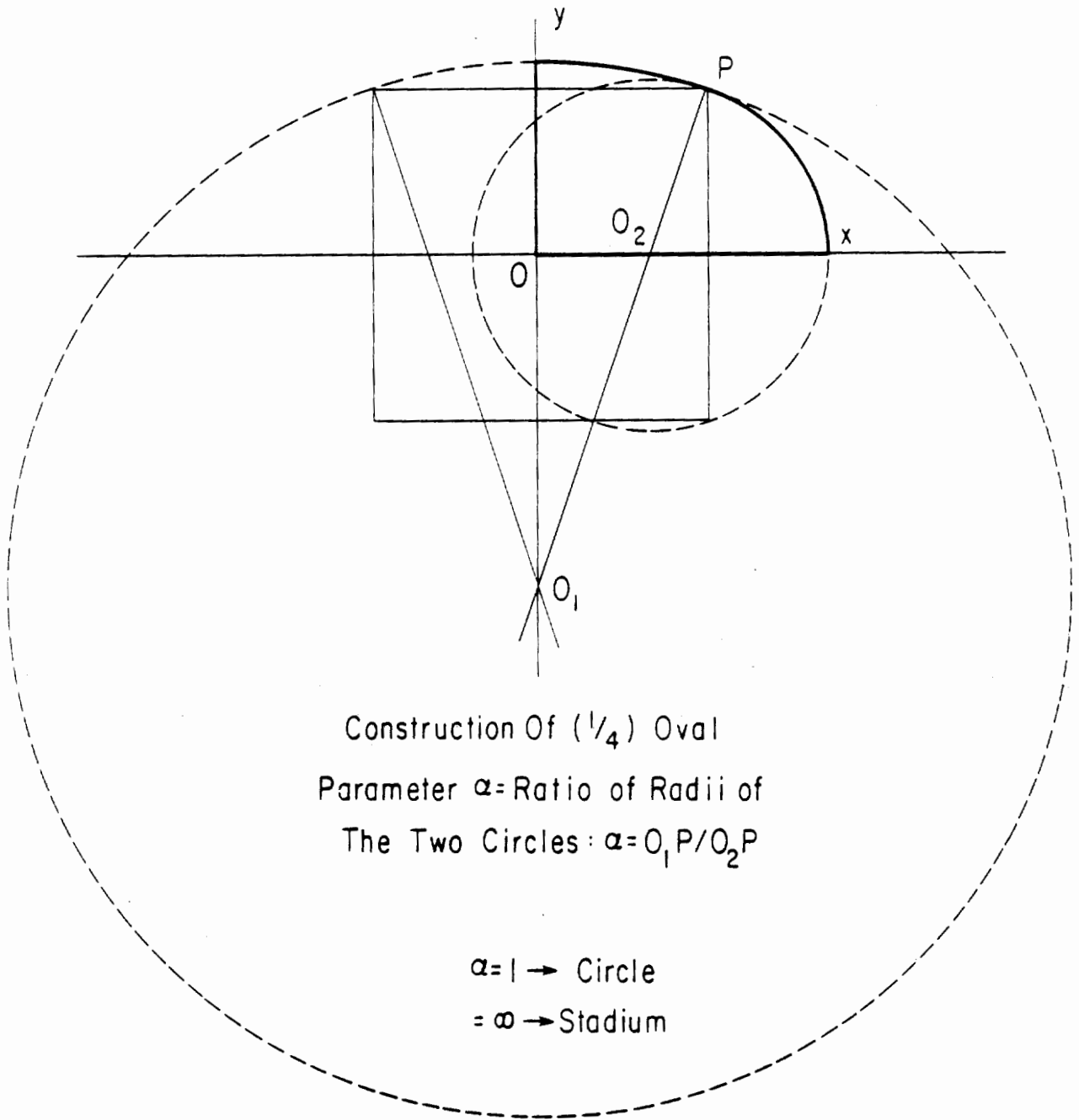


Fig. 5

85T0261

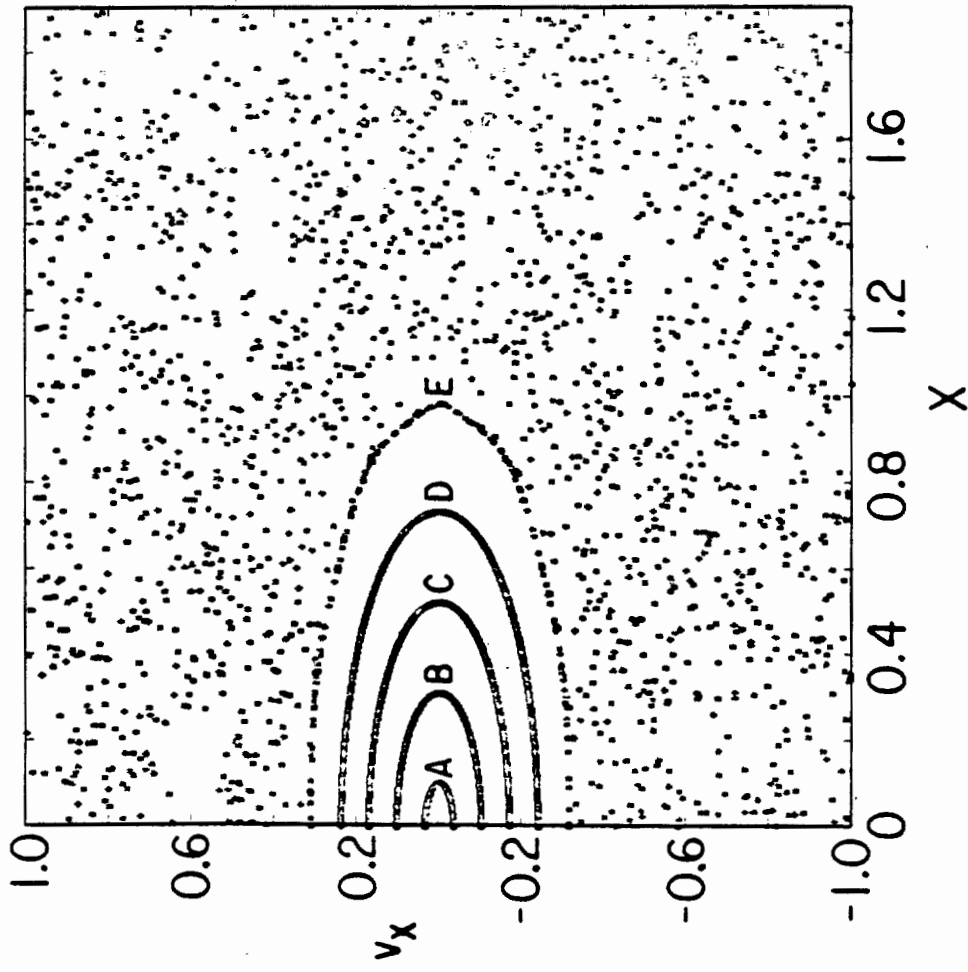
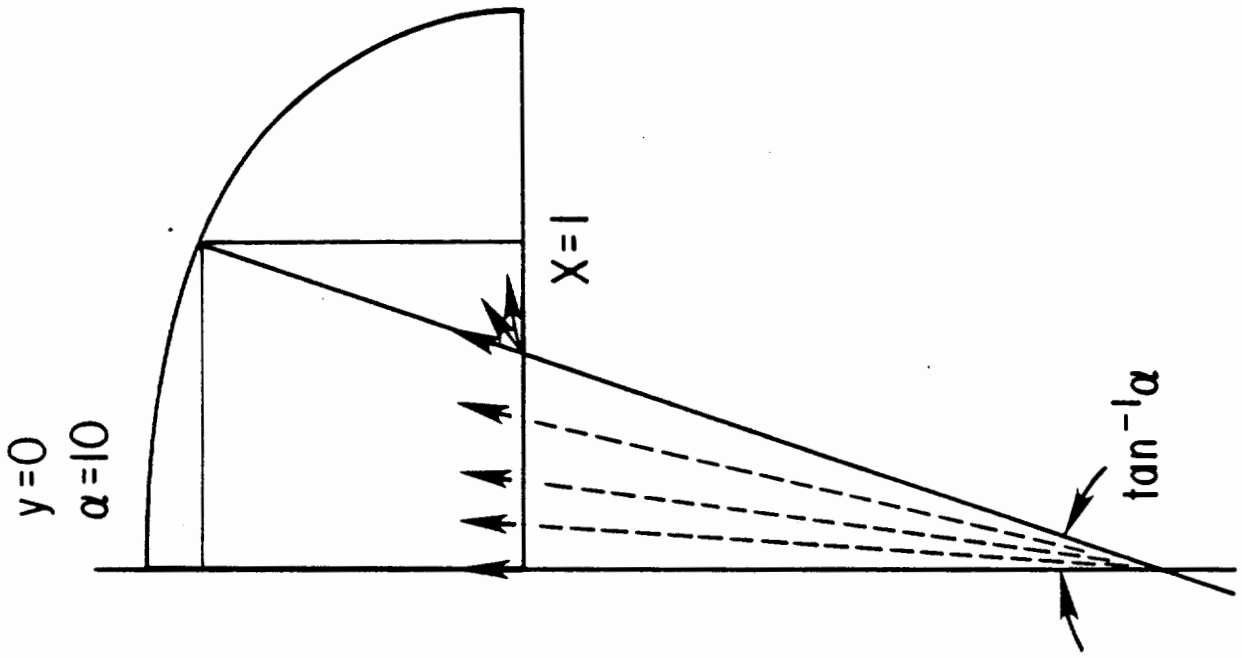


Fig. 6

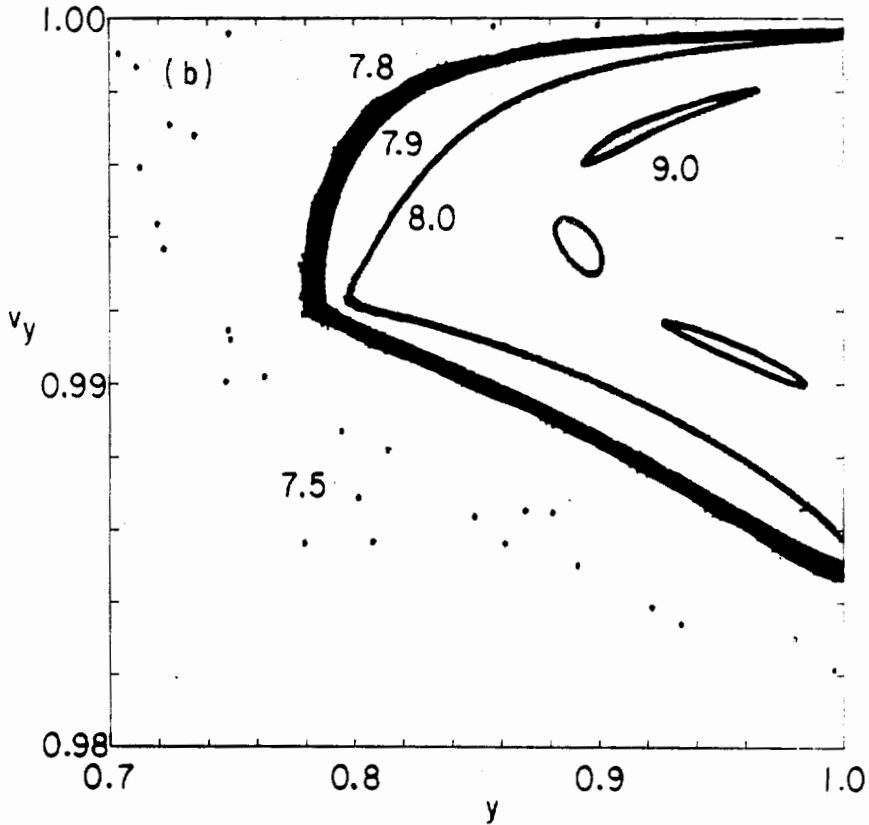
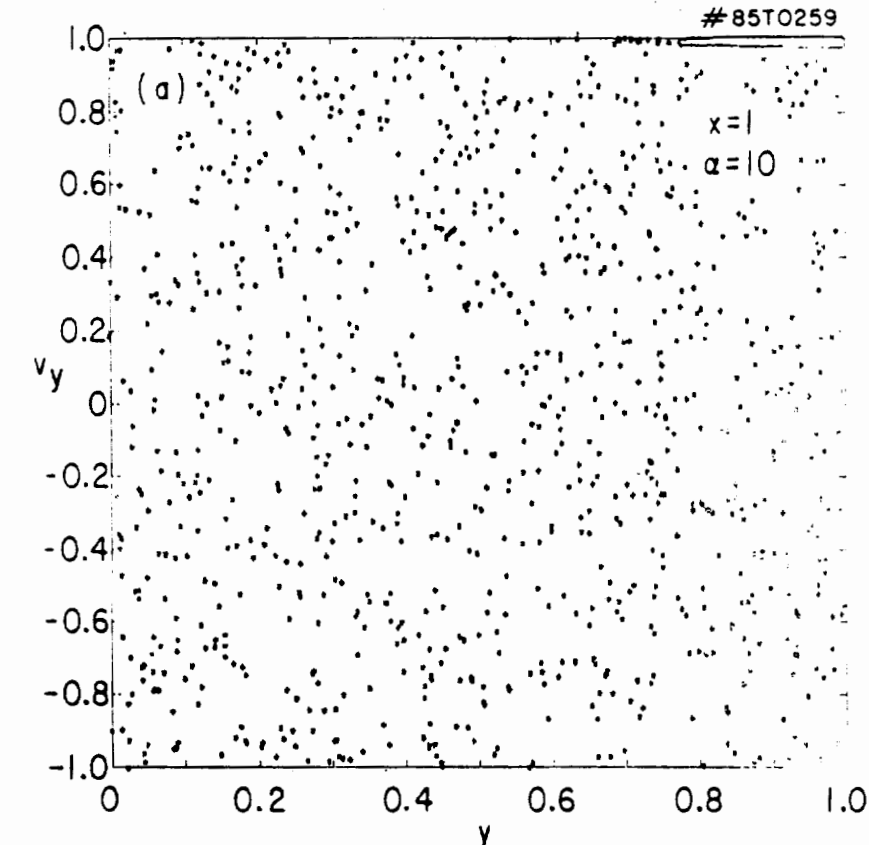


Fig. 7

#87T0106

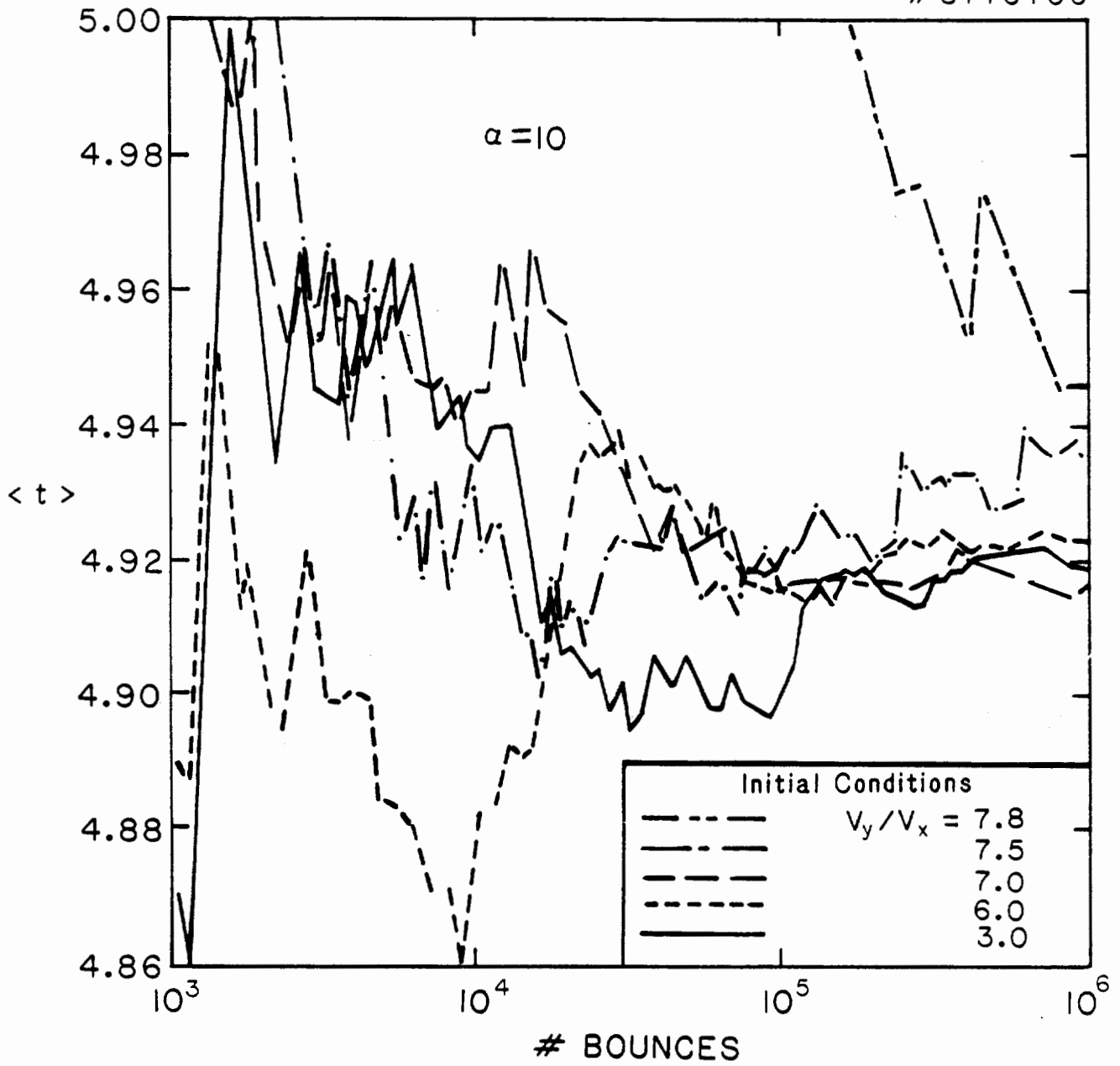


Fig. 8

#87T0107

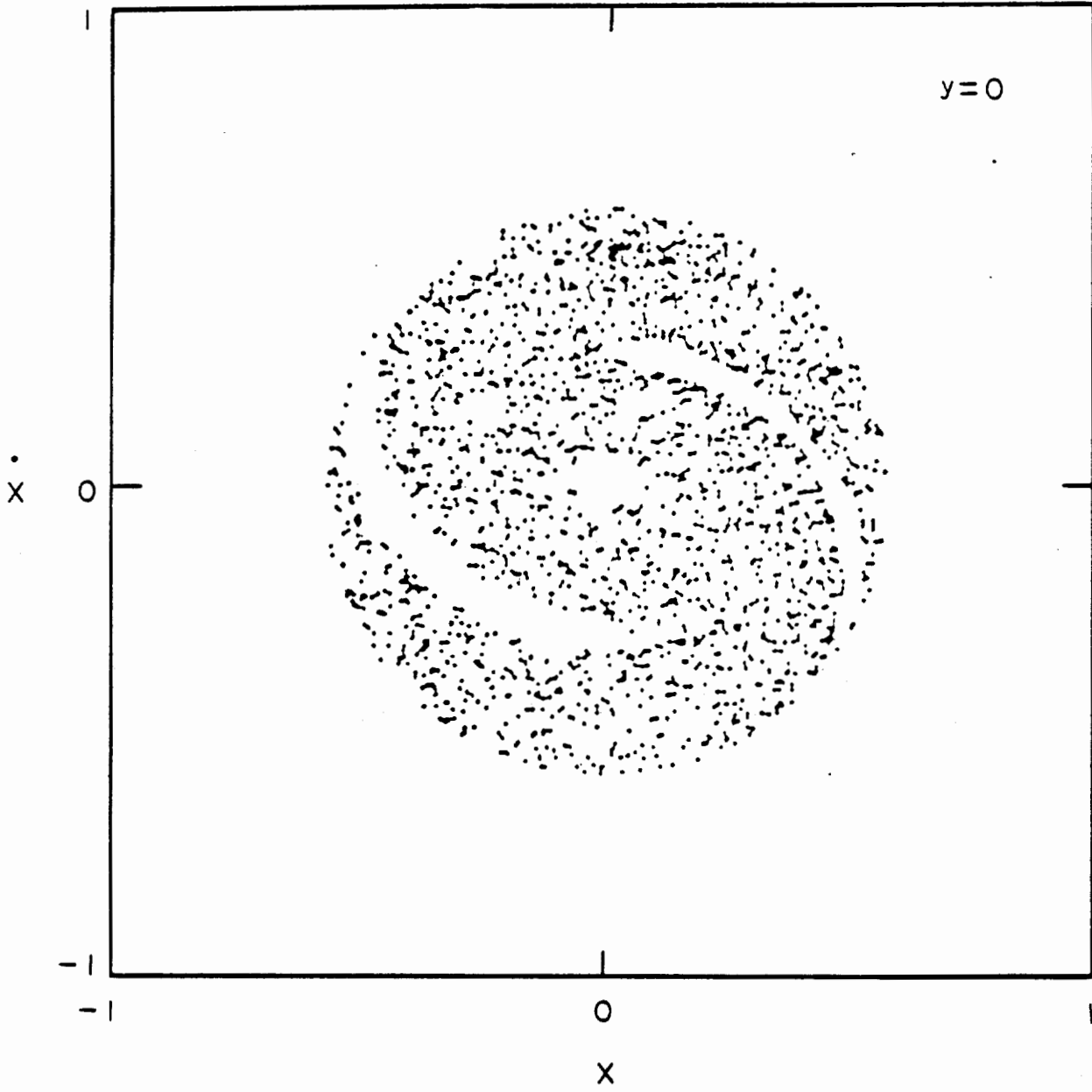


Fig. 9